

2012

Controlling a satellite dish for two way Internet communication from a moving vehicle

Peter de Boer Martinson
Iowa State University

Follow this and additional works at: <http://lib.dr.iastate.edu/etd>



Part of the [Mechanical Engineering Commons](#), and the [Robotics Commons](#)

Recommended Citation

Martinson, Peter de Boer, "Controlling a satellite dish for two way Internet communication from a moving vehicle" (2012). *Graduate Theses and Dissertations*. 12927.
<http://lib.dr.iastate.edu/etd/12927>

This Thesis is brought to you for free and open access by the Graduate College at Iowa State University Digital Repository. It has been accepted for inclusion in Graduate Theses and Dissertations by an authorized administrator of Iowa State University Digital Repository. For more information, please contact digirep@iastate.edu.

Controlling a satellite dish for two way Internet communication from a moving vehicle

by

Peter de Boer Martinson

A thesis submitted to the graduate faculty
in partial fulfillment of requirements for the degree of

MASTER OF SCIENCE

Major: Mechanical Engineering

Program of Study Committee:
Greg Luecke, Major Professor
Atul Kelkar
Gary Tuttle

Iowa State University

Ames, Iowa

2012

Copyright © Peter de Boer Martinson, 2012. All rights reserved

Table of Contents

Abstract.....	iii
Chapter 1: Introduction.....	1
Purpose.....	1
State of the Art.....	1
Chapter 2: Technical Development.....	3
Axis Rotations.....	3
The System.....	3
Measurements.....	7
Gyroscopes.....	7
Accelerometers.....	8
Signal Strength.....	9
Kalman Filter.....	12
States.....	12
State Update Equations.....	13
Output Equations.....	14
Covariances.....	14
Measurements.....	14
IMU.....	14
Signal Strength.....	16
States.....	17
Linearization.....	18
State Update Equations.....	18
Output Equations.....	19
Extended Kalman Filter.....	20
Controller.....	22
Position.....	22
Velocity.....	22
Command.....	23
Chapter 3: Simulation Results.....	24
Chapter 4: Experimental Results.....	27
Chapter 5: Conclusions.....	28
Bibliography.....	30
Appendix.....	31
Symbol Index.....	31
Output Matrix Derivatives.....	34

Abstract

In this paper a method of estimating the yaw, pitch, and roll of the satellite dish is derived. The measurements available are 3 axis accelerometers, 3 axis gyroscopes, and 3 different signal strength measurements at 3 different angles. Once the yaw, pitch, and roll states are estimated using an Extended Kalman Filter (EKF), a state feedback controller for the 3 degrees of freedom is designed.

The system achieves a precision of $\pm 0.5^\circ$ in the elevation direction, but fails to achieve this level of precision in azimuth. However, there are improvements that could reasonably be made to the system and it may perform better in the field due to more precise antennae.

Chapter 1: Introduction

Purpose

The purpose of this project is to develop a system for pointing a parabolic antenna at a satellite so as to maintain an Internet connection from a moving vehicle such as a boat, RV, or bus. Maintaining a television signal is as simple as pointing the dish within 2 degrees of the satellite in azimuth and elevation. However, an Internet connection requires that the dish must point within 0.5 degrees of the satellite, in azimuth and elevation, and the transmitter must be turned off if this level of precision is ever lost. In addition, a satellite Internet signal is linearly polarized, as opposed to circularly polarized TV signals, so the receiver and transmitter must align in the correct “skew” angle in relation to the satellite. The three degrees of freedom required for a Internet connection are azimuth, elevation, and skew. A TV signal only requires azimuth and elevation. The bulk of this paper is deriving and describing the system for estimating the yaw, pitch and roll angles, then testing and evaluating the system.

State of the Art

The current state of the art in estimating vehicle yaw, pitch, and roll is done with inertial measurement units (IMUs) and supplemental measurements. The current method of aiming satellite dishes at satellites for TV, in available consumer products, is using a circular search. Circular searches require moving the dish in a circular pattern of a diameter of at least 1 degree. The circular search will consume all of the precision required for an Internet connection and a different method is required.

The autonomous underwater vehicle, the Taipan 2, has a IMU with 3 axis accelerometers and 3 axis gyroscopes, 2 depth sensors, a Workhorse Doppler Velocity Log, as well as a GPS unit to determine the position states of the system. These were used to design a Lyapunov based diving control for the AUV [Lapierre, 2009]. The GPS measurements are used to make correction on the predicted course. The course predictions are made with the other measurements applied to linearized models around specific operating points. Controllers were designed for each model and interpolated in between operating points.

To control a rotorcraft-based unmanned aerial vehicle (RUAV) accelerations, angular velocities, linear velocities, as well as rotor velocities are measured. A dynamic system model is used to estimate the states of the vehicle from these measurements [Kim, Budiyo, et. al. , 2010]. The model consists

of rigid body dynamics, angular kinematics, and lumped rotor and stabilizer bar dynamics. The control architecture contains multiple loops. The gains were tuned in simulation.

Estimating Aerodynamic parameters (which include yaw, pitch, and roll) of aircraft is done with extended Kalman filters (EKFs) as well as unscented Kalman filters (UKFs) [Chowdhary & Jategaonkar, 2010]. The measurements used were airspeed, angle of attack, pitch position, pitch rate, pitch acceleration, longitudinal acceleration, as well as vertical acceleration. The simplified unscented Kalman filter provided little performance gain over the extended Kalman filter. The full unscented Kalman filter converged the fastest. However, both unscented Kalman filter versions are computationally expensive compared to the extended Kalman filter.

A neural network based adaptive flight control system for a high performance aircraft (F-16) has been developed. [Savran, Tasaltin, & Becerikli, 2006] Neural networks provide a method to automatically tune the controller, a PID in this case, and the state estimator. A six degree of freedom non-linear simulation of an F-16 was used to develop and test the control system. The states of the state estimator included roll, pitch, and yaw angles as well as rates.

From these papers it is apparent that supplemental measurements to gyroscopes and accelerometers are commonly used to determine vehicle states such as yaw, pitch, and roll. The difficulty in this situation is that vehicle dynamics are completely unknown and vehicle control commands are unknown. The measurements that are used must be completely contained in the satellite dish unit.

Chapter 2: Technical Development

In this section the system to be controlled will be described and the states, the filter algorithm, and the controller will be defined.

Axis Rotations

The axis rotations are the first concept to develop before anything else can be defined. We will define the physical orientation of the base of the dish with three rotations yaw, pitch, and roll. If the frame axes are applied to a car, straight ahead is positive x, to the right is positive y, and down is positive z. This conforms to ISO standard JS670.

The first rotation from the fixed frame (0 frame) is yaw (α), about the z axis in a right hand sense. The rotation matrix is denoted 1M_0 . In this notation, the right subscript is the frame the rotation applies to, and the left superscript is the frame being rotated to.

$${}^1M_0 = \begin{bmatrix} \cos(\alpha) & -\sin(\alpha) & 0 \\ \sin(\alpha) & \cos(\alpha) & 0 \\ 0 & 0 & 1 \end{bmatrix}$$

The second rotation is pitch (β), about the y axis in the 1 frame. That rotation matrix is 2M_1 .

$${}^2M_1 = \begin{bmatrix} \cos(\beta) & 0 & \sin(\beta) \\ 0 & 1 & 0 \\ -\sin(\beta) & 0 & \cos(\beta) \end{bmatrix}$$

The third and final rotation to the vehicle frame, also called frame 3, is roll (γ), about the x axis in the 2 frame. The rotation matrix is denoted 3M_2 .

$${}^3M_2 = \begin{bmatrix} 1 & 0 & 0 \\ 0 & \cos(\gamma) & -\sin(\gamma) \\ 0 & \sin(\gamma) & \cos(\gamma) \end{bmatrix}$$

The System

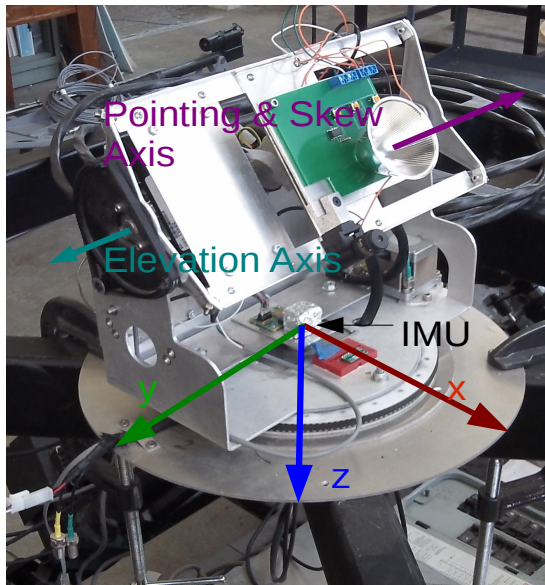
The dish has 3 motors, one for each axis of azimuth, elevation, and skew. We have chosen to mount the IMU on the rotating base of the dish, frame {3}. The reason for this is that it eases the calculations in the Kalman filter and it simplifies mounting the IMU to the dish. The azimuth motor rotates the vehicle frame, including the IMU, about the z-axis of the vehicle frame. It is important to note that the vehicle frame does not have anything to do with the 'vehicle' that the dish is mounted on

as common parlance would indicate. The elevation motor does not move the IMU, but it tilts up the antenna. The skew motor rides up and down with the elevation motor and rotates the antenna about its pointing axis.

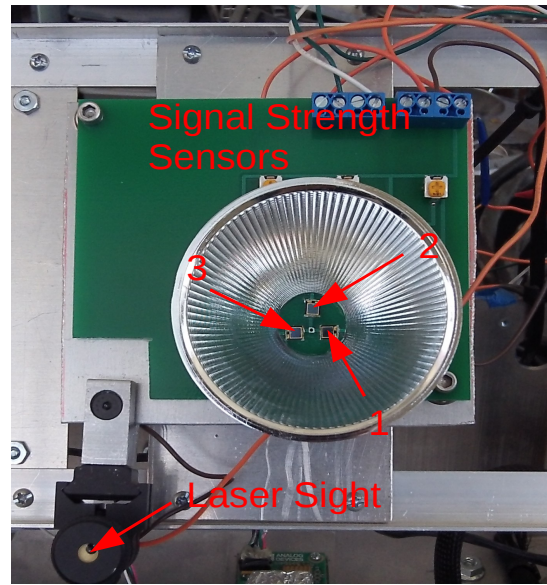
The IMU is an Analog Devices ADIS16365 [Analog Devices, 2012]. It has an accelerometer along each of the 3 perpendicular Cartesian axes, and 3 gyroscopes in the same orientation as the accelerometers. The IMU is oriented so that the x axis is coincident with the pointing vector when the elevation motor is at zero.

A K-band antenna was not supplied for this project. A substitute system using white LEDs, a parabolic reflector and photodiodes was designed. The LEDs are used to imitate the signal from the satellite and the photodiodes are used to measure the strength of the satellite signal facsimile.

The three signal strength sensors are near the focal point of a parabolic reflector. Each one is at a different angular position from the center focal point. The signal strength is measured with the LED and photodiode system. The LEDs shine from a fixed point on the laboratory wall to the parabolic reflector. The LEDs are modulated on and off at 1000 Hz. The photodiode voltages are amplified, converted to digital, then the signal is demodulated in software. There is a laser sight mounted on the dish to measure the pointing direction and how much it varies.



(a)



(b)

Figure 1: (a) the motion hardware and important axes of rotation, (b) the parabolic reflector, photodiodes, and laser sight

The LEDs light source is a set of 8 Cree MX-6S LEDs [Cree Inc, 2012]. The three photodiodes are Vishay TEMD5010X01s [Vishay, 2012]. The parabolic reflector is a Ledil F'Form Optics Barbara-S [Ledil, 2012]. Figure 1 (a) shows a picture of the motion hardware, the IMU axes and vehicle frame axes, and the motor rotation axes. Figure 1 (b) shows a close up the photodiodes used for the signal strength measurements.

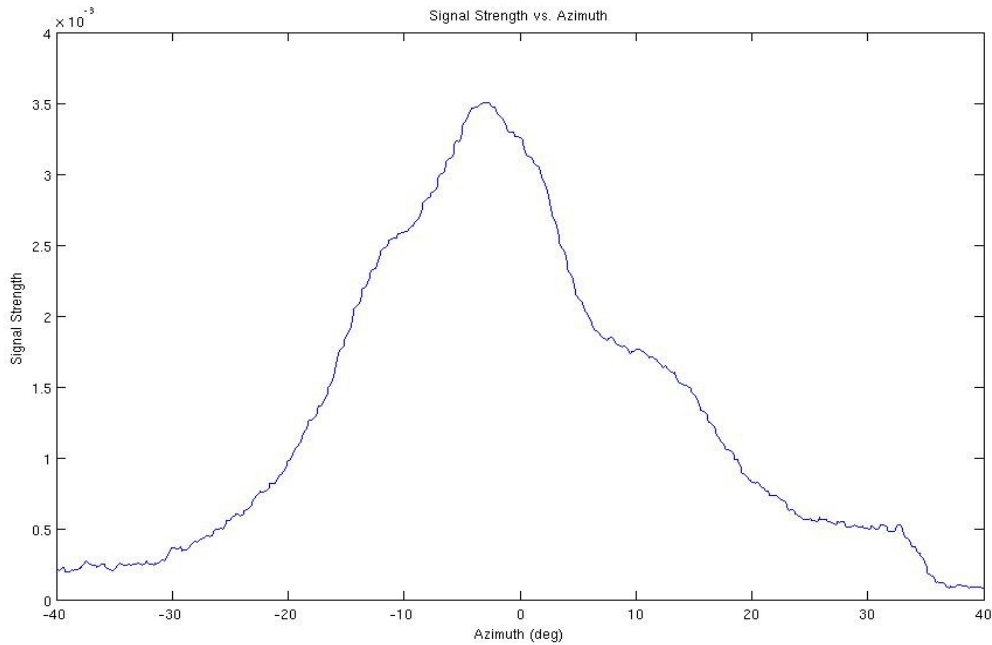


Figure 2: measured signal strength from the system

The manufacturer of the reflector provides the angular profile of light intensity for LEDs placed directly in the focal point in Figure 2.

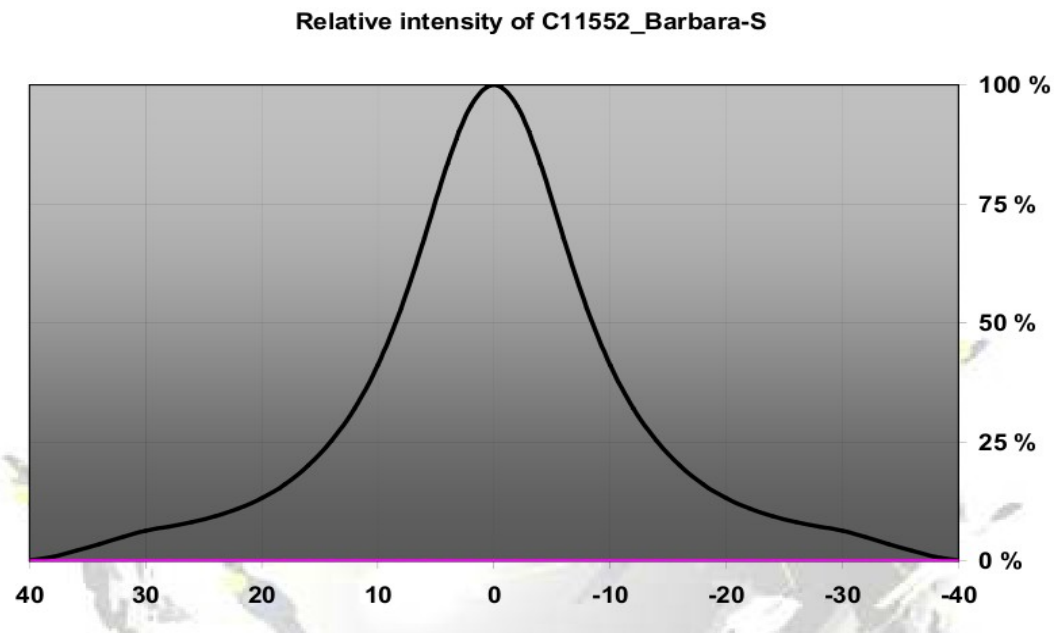


Figure 3: the relative intensity of the Barbara-S from the manufacturer

The measured intensity profile was slightly wider, as shown below in Figure 3.

The measured profile does not follow the smooth bell shape shown in the manufacturer's

diagram. The difference between the manufacturers graph and our measured graph is probably due to the fact that the LEDs are not a point source and the photodiodes are not a point sensor. This difference will likely cause systematic errors in the output estimation.

Measurements

Gyroscopes

Each gyroscope measures the angular velocity in one axis in the vehicle frame. The yaw rate ($\dot{\alpha}$) needs to be transformed from the 1 frame to the vehicle frame. And the pitch velocity ($\dot{\beta}$) needs to be translated from the 2 frame into the vehicle frame. The roll rate is already in the vehicle frame so no transformation is needed. The transformation for the yaw rate is:

$${}^3M_1 = {}^3M_2 {}^2M_1 = \begin{bmatrix} \cos(\beta) & 0 & -\sin(\beta) \\ \sin(\beta)\sin(\gamma) & \cos(\gamma) & \cos(\beta)\sin(\gamma) \\ \sin(\beta)\cos(\gamma) & -\sin(\gamma) & \cos(\beta)\cos(\gamma) \end{bmatrix}$$

The gyroscope measurements as a function of the yaw rate are:

$$\begin{bmatrix} g_x \\ g_y \\ g_z \end{bmatrix}_{\dot{\alpha}} = {}^3M_1 \begin{bmatrix} 0 \\ 0 \\ \dot{\alpha} \end{bmatrix} = \begin{bmatrix} -\dot{\alpha} \sin(\beta) \\ \dot{\alpha} \cos(\beta) \sin(\gamma) \\ \dot{\alpha} \cos(\beta) \cos(\gamma) \end{bmatrix}$$

The transform for the pitch rate is from the 2 frame to the vehicle frame (3).

$$\begin{bmatrix} g_x \\ g_y \\ g_z \end{bmatrix}_{\dot{\beta}} = {}^3M_2 \begin{bmatrix} 0 \\ \dot{\beta} \\ 0 \end{bmatrix} = \begin{bmatrix} 0 \\ \dot{\beta} \cos(\gamma) \\ \dot{\beta} \sin(\gamma) \end{bmatrix}$$

Since the roll rate is in the vehicle frame the gyroscope measurements due to the roll rate ($\dot{\gamma}$) are:

$$\begin{bmatrix} g_x \\ g_y \\ g_z \end{bmatrix}_{\dot{\gamma}} = \begin{bmatrix} \dot{\gamma} \\ 0 \\ 0 \end{bmatrix}$$

The total gyroscope readings are a sum of the roll, pitch, and yaw rates.

$$\begin{bmatrix} g_x \\ g_y \\ g_z \end{bmatrix} = \begin{bmatrix} g_x \\ g_y \\ g_z \end{bmatrix}_{\dot{\gamma}} + \begin{bmatrix} g_x \\ g_y \\ g_z \end{bmatrix}_{\dot{\beta}} + \begin{bmatrix} g_x \\ g_y \\ g_z \end{bmatrix}_{\dot{\alpha}} = \begin{bmatrix} \dot{\gamma} - \dot{\alpha} \sin(\beta) \\ \dot{\beta} \cos(\gamma) + \dot{\alpha} \cos(\beta) \sin(\gamma) \\ \dot{\beta} \sin(\gamma) + \dot{\alpha} \cos(\beta) \cos(\gamma) \end{bmatrix}$$

Accelerometers

The accelerometers will measure the gravity vector together with linear accelerations. The only linear accelerations that will be modeled in the output equations are due to rotation about a point at some distance from the origin of the vehicle frame along the z-axis. This radius will be referred to as R_z . The radius is included to capture the swaying motion of a boat if the dish is mounted on a mast. No vehicle accelerations are modeled because they are assumed to be small compared to the accelerations due to rotation. The type of vehicles the dish is intended to be mounted on are larger boats, and the lack of knowledge about how they will be moving makes modeling almost impossible.

Transforming the angular accelerations is similar to the angular velocities. The accelerometer readings from the angular accelerations are:

$$\begin{bmatrix} a_x \\ a_y \\ a_z \end{bmatrix}_{accel} = \begin{bmatrix} 0 \\ 0 \\ R_z \end{bmatrix} \times \left({}^3M_1 \begin{bmatrix} 0 \\ 0 \\ \ddot{\alpha} \end{bmatrix} + {}^3M_2 \begin{bmatrix} 0 \\ \ddot{\beta} \\ 0 \end{bmatrix} + \begin{bmatrix} \ddot{\gamma} \\ 0 \\ 0 \end{bmatrix} \right)$$

$$\begin{bmatrix} a_x \\ a_y \\ a_z \end{bmatrix}_{accel} = \begin{bmatrix} -R_z \cdot (\ddot{\beta} \cos(\gamma) + \ddot{\alpha} \cos(\beta) \sin(\gamma)) \\ R_z \cdot (\ddot{\gamma} - \ddot{\alpha} \sin(\beta)) \\ 0 \end{bmatrix}$$

The acceleration due to the centripetal force is only due to the angular velocity in the vehicle frame along the x and y axes. The rotation about the z axis is coincident with R_z , so no linear acceleration occurs. The calculation for this is below:

$$\begin{bmatrix} a_x \\ a_y \\ a_z \end{bmatrix}_{centr} = \frac{R_z^2 (g_x^2 + g_y^2)}{R_z} \cdot \hat{z}_3 = \begin{bmatrix} 0 \\ 0 \\ R_z ((\dot{\gamma} - \dot{\alpha} \sin(\beta))^2 + (\dot{\beta} \cos(\gamma) + \dot{\alpha} \cos(\beta) \sin(\gamma))^2) \end{bmatrix}$$

The last source of acceleration that is modeled is the acceleration due to gravity. The gravity vector is -9.81 m/s^2 (grav) in the z direction. The gravity vector in the fixed frame needs to be transformed into the vehicle frame.

$$\begin{bmatrix} a_x \\ a_y \\ a_z \end{bmatrix}_{grav} = {}^3M_0 \begin{bmatrix} 0 \\ 0 \\ grav \end{bmatrix} = \begin{bmatrix} -grav \cdot \sin(\beta) \\ grav \cdot \cos(\beta) \sin(\gamma) \\ grav \cdot \cos(\beta) \cos(\gamma) \end{bmatrix}$$

So, the total accelerometer readings (a) are:

$$\begin{bmatrix} a_x \\ a_y \\ a_z \end{bmatrix} = \begin{bmatrix} a_x \\ a_y \\ a_z \end{bmatrix}_{accel} + \begin{bmatrix} a_x \\ a_y \\ a_z \end{bmatrix}_{centr} + \begin{bmatrix} a_x \\ a_y \\ a_z \end{bmatrix}_{grav}$$

$$\begin{bmatrix} a_x \\ a_y \\ a_z \end{bmatrix} = \begin{bmatrix} -R_z \cdot (\ddot{\beta} \cos(\gamma) + \ddot{\alpha} \cos(\beta) \sin(\gamma)) - grav \cdot \sin(\beta) \\ R_z \cdot (\ddot{\gamma} - \ddot{\alpha} \sin(\beta)) + grav \cdot \cos(\beta) \sin(\gamma) \\ R_z ((\dot{\gamma} - \dot{\alpha} \sin(\beta))^2 + (\dot{\beta} \cos(\gamma) + \dot{\alpha} \cos(\beta) \sin(\gamma))^2) + grav \cdot \cos(\beta) \cos(\gamma) \end{bmatrix}$$

Signal Strength

The signal strength (SS) is measured at three different angular locations relative to the pointing vector of the dish. They have specific locations on the hardware system shown in Figure 1(b). For this analysis we can assign them arbitrary locations. They will be labeled as follows:

$$\begin{aligned} SS_1 \text{ location} &= (az_1, el_1) \\ SS_2 \text{ location} &= (az_2, el_2) \\ SS_3 \text{ location} &= (az_3, el_3) \end{aligned}$$

The location of each signal strength measurement is relative to the nominal pointing location and skew of the dish. The skew angle rotates each location (az, el) about the nominal pointing location. The expected signal strength of the nominal pointing location (p) is found using a theoretical representation of the signal.

$$SS_{nom} = A \exp \left[\frac{-(p_{az} - s_{az})^2}{2\sigma^2} - \frac{(p_{el} - s_{el})^2}{2\sigma^2} \right]$$

Where A is the peak signal strength, 's' is the satellite location, and σ is the “standard deviation” or width of the signal strength bell curve. Modeling the signal strength with a Gaussian function will be justified later. Accepting the skew angle as 0, adding in the location of signal strength measurement 1 yields:

$$SS_1 = A \exp \left[-\frac{(p_{az} + az_1 - s_{az})^2}{2\sigma^2} - \frac{(p_{el} + el_1 - s_{el})^2}{2\sigma^2} \right]$$

Then (az_1, el_1) must be rotated about (p_{az}, p_{el}) by the skew angle (p_{sk}). The process for this is shown in Figure 4.

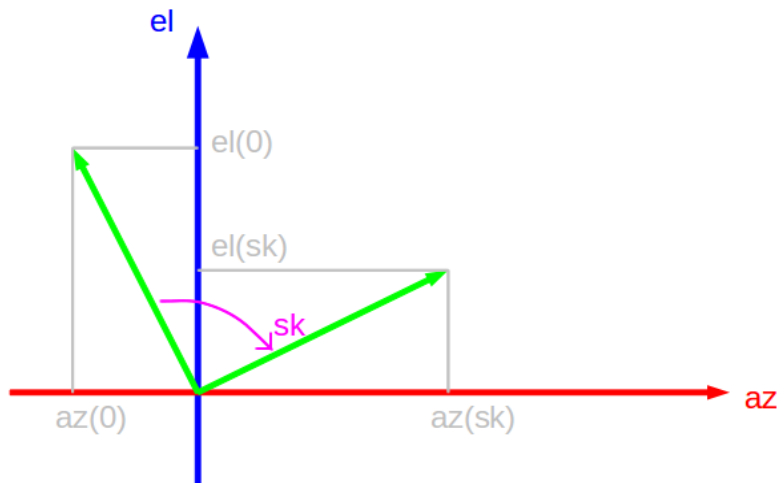


Figure 4: how the signal strength measurements are rotated about the nominal pointing vector

Including the rotated signal strength measurements yields:

$$SS_1 = A \exp \left[-\frac{(p_{az} + az_1 \cos(p_{sk}) + el_1 \sin(p_{sk}) - s_{az})^2}{2\sigma^2} - \frac{(p_{el} + el_1 \cos(p_{sk}) - az_1 \sin(p_{sk}) - s_{el})^2}{2\sigma^2} \right]$$

The other signal strength measurements are similarly:

$$SS_2 = A \exp \left[-\frac{(p_{az} + az_2 \cos(p_{sk}) + el_2 \sin(p_{sk}) - s_{az})^2}{2\sigma^2} - \frac{(p_{el} + el_2 \cos(p_{sk}) - az_2 \sin(p_{sk}) - s_{el})^2}{2\sigma^2} \right]$$

$$SS_3 = A \exp \left[-\frac{(p_{az} + az_3 \cos(p_{sk}) + el_3 \sin(p_{sk}) - s_{az})^2}{2\sigma^2} - \frac{(p_{el} + el_3 \cos(p_{sk}) - az_3 \sin(p_{sk}) - s_{el})^2}{2\sigma^2} \right]$$

Next we will derive how the pointing location is determined. The pointing location in the vehicle frame is a function of the elevation motor position (θ).

$$p_3 = \begin{bmatrix} \cos(\theta) \\ 0 \\ -\sin(\theta) \end{bmatrix}$$

Then, perform the inverse of the roll kinematics relation:

$${}^2M_3 = \begin{bmatrix} 1 & 0 & 0 \\ 0 & \cos(\gamma) & \sin(\gamma) \\ 0 & -\sin(\gamma) & \cos(\gamma) \end{bmatrix}$$

Then, the inverse of the pitch kinematics:

$${}^1M_2 = \begin{bmatrix} \cos(\beta) & 0 & -\sin(\beta) \\ 0 & 1 & 0 \\ \sin(\beta) & 0 & \cos(\beta) \end{bmatrix}$$

Finally, the inverse of the yaw kinematics:

$${}^0M_1 = \begin{bmatrix} \cos(\alpha) & \sin(\alpha) & 0 \\ -\sin(\alpha) & \cos(\alpha) & 0 \\ 0 & 0 & 1 \end{bmatrix}$$

All together:

$${}^0M_3 = {}^0M_1 {}^1M_2 {}^2M_3$$

$${}^0M_3 = \begin{bmatrix} \cos(\beta)\cos(\alpha) & \sin(\beta)\cos(\alpha)\sin(\gamma) - \sin(\alpha)\cos(\gamma) & \sin(\alpha)\sin(\gamma) + \sin(\beta)\cos(\alpha)\cos(\gamma) \\ \cos(\beta)\sin(\alpha) & \cos(\alpha)\cos(\gamma) + \sin(\beta)\sin(\alpha)\sin(\gamma) & \sin(\beta)\sin(\alpha)\cos(\gamma) - \cos(\alpha)\sin(\gamma) \\ -\sin(\beta) & \cos(\beta)\sin(\gamma) & \cos(\beta)\cos(\gamma) \end{bmatrix}$$

So the pointing vector in the fixed frame is:

$$p_0 = {}^0M_3 p_3$$

$$\begin{bmatrix} p_{0x} \\ p_{0y} \\ p_{0z} \end{bmatrix} = \begin{bmatrix} \cos(\beta)\cos(\alpha)\cos(\theta) - \sin(\theta)(\sin(\alpha)\sin(\gamma) + \sin(\beta)\cos(\alpha)\cos(\gamma)) \\ \sin(\theta)(\cos(\alpha)\sin(\gamma) - \sin(\beta)\sin(\alpha)\cos(\gamma)) + \cos(\beta)\cos(\theta)\sin(\alpha) \\ -\sin(\beta)\cos(\theta) - \cos(\beta)\sin(\theta)\cos(\gamma) \end{bmatrix}$$

Finally, calculate the azimuth and elevation angle of the pointing vector:

$$p_{az} = \tan^{-1}\left(\frac{p_{0y}}{p_{0x}}\right)$$

$$p_{el} = -\tan^{-1}\left(\frac{p_{0z}}{\sqrt{p_{0x}^2 + p_{0y}^2}}\right)$$

The skew angle (p_{sk}) is the skew motor angle and the roll component in the pointing vector.

Figure 5 shows how this is derived.

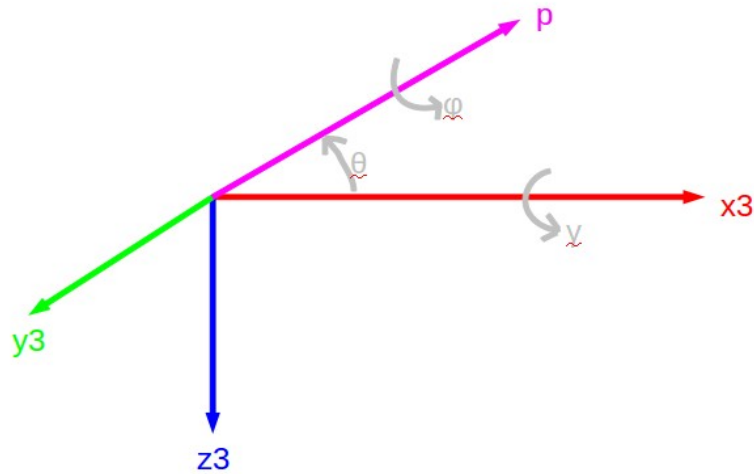


Figure 5: the angles and vectors involved in the skew angle of the dish

The formula for the skew angle is:

$$p_{sk} = \gamma \cos(\theta) + \phi$$

Where ϕ is the skew motor position.

Once all the frames of reference are defined and measurements modeled, development of the state observer can begin.

Kalman Filter

States

A good clue as to what states should be included is to look at what is to be estimated and the variables in the measurements. The states that were chosen were:

$$\ddot{\gamma} = \frac{d^2 \gamma}{dt^2}; \ddot{\beta} = \frac{d^2 \beta}{dt^2}; \ddot{\alpha} = \frac{d^2 \alpha}{dt^2}; \dot{\gamma} = \frac{d\gamma}{dt}; \dot{\beta} = \frac{d\beta}{dt}; \dot{\alpha} = \frac{d\alpha}{dt}; \gamma = \text{roll}; \beta = \text{pitch}; \alpha = \text{yaw};$$

$R_z = \text{radius of rotation along } z \text{ axis}; A = \text{amplitude of signal strength peak}$

State Update Equations

The accelerations $(\ddot{\gamma}, \ddot{\beta}, \ddot{\alpha})$ are all modeled as constants with a high degree of uncertainty. The velocities $(\dot{\gamma}, \dot{\beta}, \dot{\alpha})$ are integrations of the accelerations, and the positions (γ, β, α) are integrations of the velocities. R_z and A are modeled as constants. The inputs are the elevation motor position and the skew motor position, but they are not variables in the state update equations. The state update equations are:

$$\begin{aligned}
 \ddot{\gamma}_{k+1} &= \ddot{\gamma}_k + w_{1k} \\
 \ddot{\beta}_{k+1} &= \ddot{\beta}_k + w_{2k} \\
 \ddot{\alpha}_{k+1} &= \ddot{\alpha}_k + w_{3k} \\
 \dot{\gamma}_{k+1} &= \dot{\gamma}_k + T \ddot{\gamma}_k + w_{4k} \\
 \dot{\beta}_{k+1} &= \dot{\beta}_k + T \ddot{\beta}_k + w_{5k} \\
 \dot{\alpha}_{k+1} &= \dot{\alpha}_k + T \ddot{\alpha}_k + w_{6k} \\
 \gamma_{k+1} &= \gamma_k + T \dot{\gamma}_k + \frac{T^2}{2} \ddot{\gamma}_k + w_{7k} \\
 \beta_{k+1} &= \beta_k + T \dot{\beta}_k + \frac{T^2}{2} \ddot{\beta}_k + w_{8k} \\
 \alpha_{k+1} &= \alpha_k + T \dot{\alpha}_k + \frac{T^2}{2} \ddot{\alpha}_k + w_{9k} \\
 R_{z_{k+1}} &= R_{z_k} + w_{10k} \\
 A_{k+1} &= A_k + w_{11k}
 \end{aligned}$$

Where k represents the current time step and $k+1$ is the next. T is the time step period. The w variable represents the error.

Output Equations

These are taken almost directly from the measurement equations.

$$\begin{aligned}
 & \text{gyros} \begin{bmatrix} g_{xk} = \dot{\gamma}_k - \dot{\alpha}_k \sin(\beta_k) + v_{1k} \\ g_{yk} = \dot{\beta}_k \cos(\gamma_k) + \dot{\alpha}_k \cos(\beta_k) \sin(\gamma_k) + v_{2k} \\ g_{zk} = \dot{\beta}_k \sin(\gamma_k) + \dot{\alpha}_k \cos(\beta_k) \cos(\gamma_k) + v_{3k} \end{bmatrix} \\
 & \text{accels} \begin{bmatrix} a_{xk} = -R_{zk} \cdot (\ddot{\beta}_k \cos(\gamma_k) + \ddot{\alpha}_k \cos(\beta_k) \sin(\gamma_k)) - \text{grav} \cdot \sin(\beta_k) + v_{4k} \\ a_{yk} = R_{zk} \cdot (\ddot{\gamma}_k - \ddot{\alpha}_k \sin(\beta_k)) + \text{grav} \cdot \cos(\beta_k) \sin(\gamma_k) + v_{5k} \\ a_{zk} = R_{zk} \cdot ((\dot{\gamma}_k - \dot{\alpha}_k \sin(\beta_k))^2 + (\dot{\beta}_k \cos(\gamma_k) + \dot{\alpha}_k \cos(\beta_k) \sin(\gamma_k))^2) + \text{grav} \cdot \cos(\beta_k) \cos(\gamma_k) + v_{6k} \end{bmatrix} \\
 & SS_{1k} = A_k \exp \left[-\frac{(p_{az} + az_1 \cos(p_{sk}) + el_1 \sin(p_{sk}) - s_{az})^2}{2\sigma^2} - \frac{(p_{el} + el_1 \cos(p_{sk}) - az_1 \sin(p_{sk}) - s_{el})^2}{2\sigma^2} \right] + v_{7k} \\
 & SS_{2k} = A_k \exp \left[-\frac{(p_{az} + az_2 \cos(p_{sk}) + el_2 \sin(p_{sk}) - s_{az})^2}{2\sigma^2} - \frac{(p_{el} + el_2 \cos(p_{sk}) - az_2 \sin(p_{sk}) - s_{el})^2}{2\sigma^2} \right] + v_{8k} \\
 & SS_{3k} = A_k \exp \left[-\frac{(p_{az} + az_3 \cos(p_{sk}) + el_3 \sin(p_{sk}) - s_{az})^2}{2\sigma^2} - \frac{(p_{el} + el_3 \cos(p_{sk}) - az_3 \sin(p_{sk}) - s_{el})^2}{2\sigma^2} \right] + v_{9k}
 \end{aligned}$$

The variables p_{az} , p_{el} , and p_{sk} are intermediate variables to shorten the written equations for the signal strengths. Calculating those intermediate variables have been shown above. And in this case, the v variables represent the error.

Covariances

Measurements

The variances for the measurements were determined by calculating the variances between the actual measurements and the output for known states from the model. The initial covariance matrices are all assumed to be diagonal for convenience.

IMU

To measure the IMU noise, the IMU was oriented on the same axes as the motion base so that the IMU's yaw, pitch, and roll will be the same as the motion base's. Then the motion base was rolled, pitched, and yawed in a sinusoidal pattern about a point 1 meter below the IMU. The sinusoids are summarized as follows:

Yaw: 0.12 radians @ 0.14 Hertz

Pitch: 0.18 radians @ 0.11 Hertz

Roll: 0.16 radians @ 0.13 Hertz

$R_z = 1$ meter

These numbers were picked toward the limit of the motion base's range of motion. The output model compared to the measurements are shown in Figure 6 below.

The variances for each IMU measurement are:

$$R_{x\text{-gyro}} = 5.3494\text{e-}05$$

$$R_{y\text{-gyro}} = 5.9099\text{e-}05$$

$$R_{z\text{-gyro}} = 9.6015\text{e-}05$$

$$R_{x\text{-accel}} = 0.0227$$

$$R_{y\text{-accel}} = 0.0170$$

$$R_{z\text{-accel}} = 0.0447$$

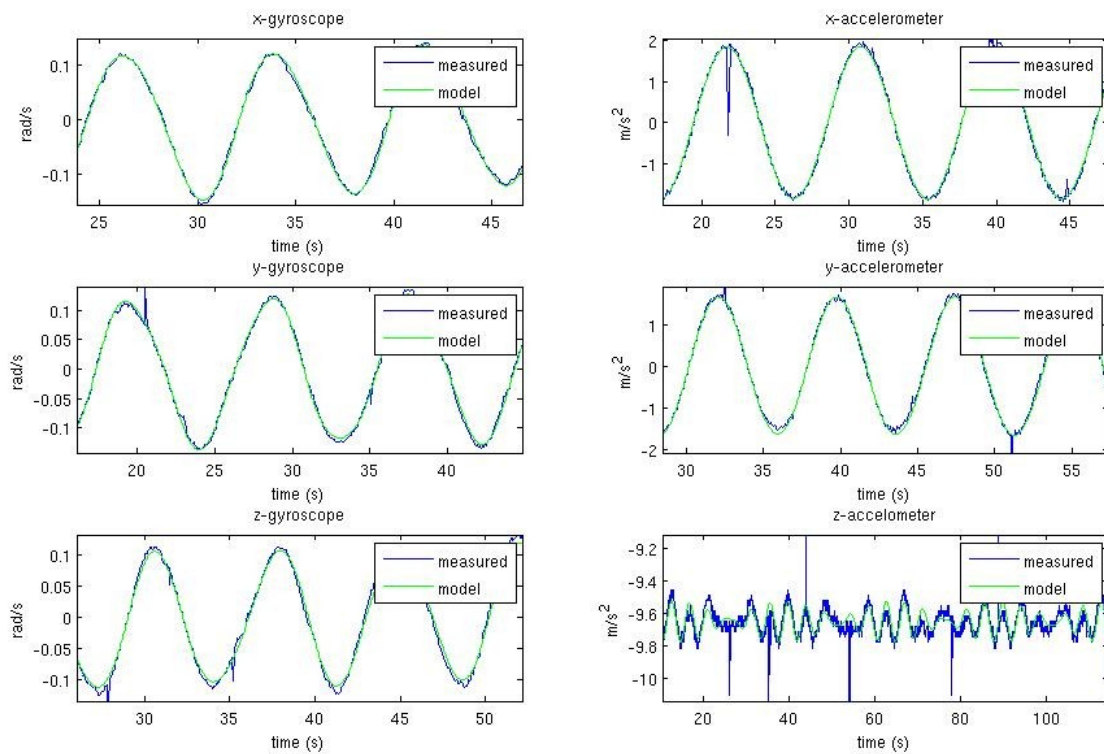


Figure 6: a comparison of the model estimate and the IMU measurements

Signal Strength

The signal strength was measured by moving the elevation motor from 0 to approximately 80 degrees in 9 different azimuth positions, keeping the skew angle zero. Each signal strength measurement was recorded at each elevation and azimuth position. From this data the relative signal strength measurement positions, the signal strength spread, and amplitude were estimated.

A “noise” component was added because the measurement did not drop to zero as the dish was pointed further and further away from the light source. This does not change any derivative calculations in the Kalman filter, so we can continue with implementation. The equation used for each of the 3 measurements in the model was:

$$SS = A \exp \left[-\frac{(p_{az} + az - s_{az})^2}{2\sigma^2} - \frac{(p_{el} + el - s_{el})^2}{2\sigma^2} \right] + noise$$

To demonstrate the reasonableness of this approximation, Figure 7 below shows the best fitting signal strength measurement.

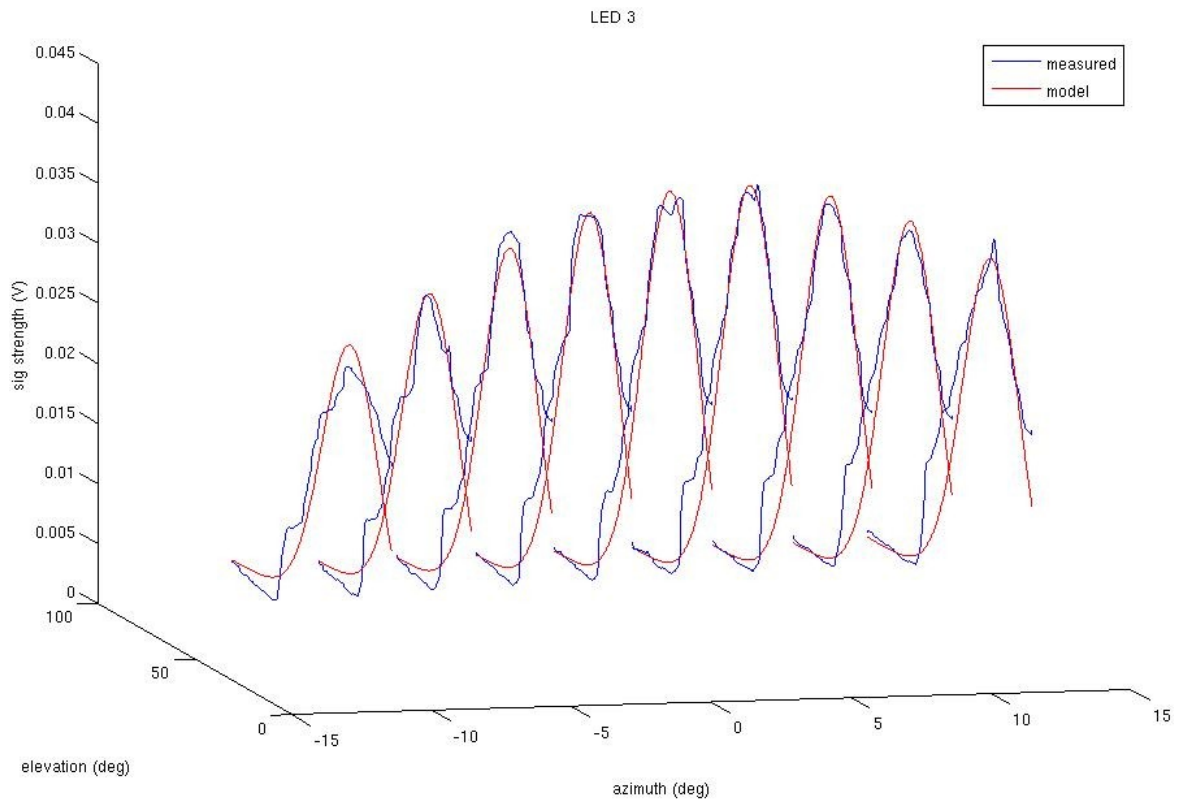


Figure 7: Gaussian model and measured signal strength

The variances for each measurement are:

$$R_1 = 1.107e-5$$

$$R_2 = 0.713e-5$$

$$R_3 = 1.125e-5$$

The relative locations to the nominal pointing direction of each signal strength measurement were determined, mostly by trial and error, to be: (azimuth, elevation) in degrees

$$SS_1 (1, 1) ; SS_2 (1, -3) ; SS_3 (-3, 1)$$

States

The state update covariances were set up to load most of the uncertainty on the accelerations and have the integrations be very certain. The specific variances will be tuned heuristically. The covariances of the “constants”, R_z and A , will be tuned so that they do not follow the oscillation of the vehicle but do not take an unacceptable amount of time to converge.

Linearization

State Update Equations

The state update equations are already linear. Converting them to matrix form is done below. T represents the time period between updates.

$$\begin{bmatrix} \ddot{\gamma} \\ \ddot{\beta} \\ \ddot{\alpha} \\ \dot{\gamma} \\ \dot{\beta} \\ \dot{\alpha} \\ \gamma \\ \beta \\ \alpha \\ R_z \\ A \end{bmatrix}_{k+1} = \frac{T^2}{2} \begin{bmatrix} 1 & 0 & 0 & 0 & 0 & 0 & 0 & 0 & 0 & 0 & 0 \\ 0 & 1 & 0 & 0 & 0 & 0 & 0 & 0 & 0 & 0 & 0 \\ 0 & 0 & 1 & 0 & 0 & 0 & 0 & 0 & 0 & 0 & 0 \\ T & 0 & 0 & 1 & 0 & 0 & 0 & 0 & 0 & 0 & 0 \\ 0 & T & 0 & 0 & 1 & 0 & 0 & 0 & 0 & 0 & 0 \\ 0 & 0 & T & 0 & 0 & 1 & 0 & 0 & 0 & 0 & 0 \\ 0 & 0 & 0 & T & 0 & 0 & 1 & 0 & 0 & 0 & 0 \\ 0 & \frac{T^2}{2} & 0 & 0 & T & 0 & 0 & 1 & 0 & 0 & 0 \\ 0 & 0 & \frac{T^2}{2} & 0 & 0 & T & 0 & 0 & 1 & 0 & 0 \\ 0 & 0 & 0 & 0 & 0 & 0 & 0 & 0 & 1 & 0 & 0 \\ 0 & 0 & 0 & 0 & 0 & 0 & 0 & 0 & 0 & 0 & 1 \end{bmatrix} \begin{bmatrix} \ddot{\gamma} \\ \ddot{\beta} \\ \ddot{\alpha} \\ \dot{\gamma} \\ \dot{\beta} \\ \dot{\alpha} \\ \gamma \\ \beta \\ \alpha \\ R_z \\ A \end{bmatrix}_k + \begin{bmatrix} w_1 \\ w_2 \\ w_3 \\ w_4 \\ w_5 \\ w_6 \\ w_7 \\ w_8 \\ w_9 \\ w_{10} \\ w_{11} \end{bmatrix}_k$$

Output Equations

To write and understand the Jacobian of the output equations, the shorter derivatives will be directly in the matrix and the longer derivatives will be in the Appendix.

$$H_k = R_{Zk} \begin{pmatrix}
 0 & 0 & 0 & 1 & 0 & \frac{dg_{xk}}{d\dot{\alpha}_k} & 0 & \frac{dg_{xk}}{d\beta_k} & 0 & 0 & 0 \\
 0 & 0 & 0 & 0 & \cos(\gamma_k) & \frac{dg_{yk}}{\dot{\alpha}_k} & \frac{dg_{yk}}{d\gamma_k} & \frac{dg_{yk}}{d\beta_k} & 0 & 0 & 0 \\
 0 & 0 & 0 & 0 & \sin(\gamma_k) & \frac{dg_{zk}}{d\dot{\alpha}_k} & \frac{dg_{zk}}{d\gamma_k} & \frac{dg_{zk}}{d\beta_k} & 0 & 0 & 0 \\
 0 & \frac{da_{xk}}{d\ddot{\beta}_k} & \frac{da_{xk}}{d\ddot{\alpha}_k} & 0 & 0 & 0 & \frac{da_{xk}}{d\gamma_k} & \frac{da_{xk}}{d\beta_k} & 0 & \frac{da_{xk}}{dR_{Zk}} & 0 \\
 R_{Zk} & 0 & \frac{da_{yk}}{d\ddot{\alpha}_k} & 0 & 0 & 0 & \frac{da_{yk}}{d\gamma_k} & \frac{da_{yk}}{d\beta_k} & 0 & 0 & 0 \\
 0 & 0 & 0 & \frac{da_{zk}}{d\dot{\gamma}_k} & \frac{da_{zk}}{d\dot{\beta}_k} & \frac{da_{zk}}{d\dot{\alpha}_k} & \frac{da_{zk}}{d\gamma_k} & \frac{da_{zk}}{d\beta_k} & 0 & \frac{da_{zk}}{dR_{Zk}} & 0 \\
 0 & 0 & 0 & 0 & 0 & 0 & \frac{dSS_{1k}}{d\gamma_k} & \frac{dSS_{1k}}{d\beta_k} & \frac{dSS_{1k}}{d\alpha_k} & 0 & \frac{dSS_{1k}}{dA_k} \\
 0 & 0 & 0 & 0 & 0 & 0 & \frac{dSS_{2k}}{d\gamma_k} & \frac{dSS_{2k}}{d\beta_k} & \frac{dSS_{2k}}{d\alpha_k} & 0 & \frac{dSS_{2k}}{dA_k} \\
 0 & 0 & 0 & 0 & 0 & 0 & \frac{dSS_{3k}}{d\gamma_k} & \frac{dSS_{3k}}{d\beta_k} & \frac{dSS_{3k}}{d\alpha_k} & 0 & \frac{dSS_{3k}}{dA_k}
 \end{pmatrix}$$

Extended Kalman Filter

The standard Kalman filter is for optimally estimating the states of a linear system where the measurements contain Gaussian noise. The system in state space is represented as:

$$\begin{aligned}x_{k+1} &= F_k x_k + B_k u_k + W_k \\ y_k &= H_k x_k + D_k u_k + V_k\end{aligned}$$

The Kalman filter algorithm then is as follows:

Step 1: $\hat{x}_{k/k-1} = F_k \hat{x}_{k-1/k-1} + B_k u_k$ “a priori state estimate”

Step 2: $P_{k/k-1} = F_k P_{k-1/k-1} F_k^T + Q_k$ “a priori state covariance”

Step 3: $\tilde{y}_k = y_k - (H_k \hat{x}_{k/k-1} + D_k u_k)$ “measurement residual calculation”

Step 4: $S_k = H_k P_{k/k-1} H_k^T + R_k$ “measurement residual covariance”

Step 5: $K_k = P_{k/k-1} H_k^T S_k^{-1}$ “optimal Kalman gains”

Step 6: $\hat{x}_{k/k} = \hat{x}_{k/k-1} + K_k \tilde{y}_k$ “posteriori state estimate”

Step 7: $P_{k/k} = (I - K_k H_k) P_{k/k-1}$ “posteriori state covariance”

In this case, the system is represented by:

$$\begin{aligned}x_{k+1} &= F x_k + W_k \\ y_k &= h(x_k, u_k) + V_k\end{aligned}$$

Note that $B = 0$ in this system and that the output is non-linearly related to the states and the input. Also, the F matrix is constant. The extended Kalman filter in this case is the following:

Step 1: $\hat{x}_{k/k-1} = F \hat{x}_{k-1/k-1}$

Step 2: $P_{k/k-1} = F P_{k-1/k-1} F^T + Q$

Step 3: $\tilde{y}_k = y_k - h(\hat{x}_{k/k-1}, u_k)$

Step 3': $H_k = \frac{\delta h(\hat{x}_{k/k-1}, u_k)}{\delta \hat{x}_{k/k-1}}$ “calculate the Jacobian of the output equations”

$$\text{Step 4: } S_k = H_k P_{k/k-1} H_k^T + R$$

$$\text{Step 5: } K_k = P_{k/k-1} H_k^T S_k^{-1}$$

$$\text{Step 6: } \hat{x}_{k/k} = \hat{x}_{k/k-1} + K_k \tilde{y}_k$$

$$\text{Step 7: } P_{k/k} = (I - K_k H_k) P_{k/k-1}$$

Note that the matrix S_k is a 9x9 matrix and it is inverted in Step 5. This is computationally expensive. The matrix inversion can be avoided if the R matrix is diagonal or it is constant. (It can be diagonalized before running the filter if it is constant.) If in each time step the measurements are applied one at a time, then the H matrix becomes a row vector and the S matrix becomes a 1x1 matrix and inverting it is simple. The R matrix in this case is both diagonal and constant. [Simon, 2006] So, the algorithm becomes:

$$\text{Step 1: } \hat{x}_{k/k-1} = F \hat{x}_{k-1/k-1}$$

$$\text{Step 2: } P_{k/k-1} = F P_{k-1/k-1} F^T + Q$$

for $r = 1$ through 9 { “9 is the number of measurements”

$$\text{Step 3: } \tilde{y}_k = y(r)_k - h(r)(\hat{x}_{k/k-1}, u_k) \quad \text{“residual of the } r^{\text{th}} \text{ measurement”}$$

$$\text{Step 3': } H_k = \frac{\delta h(r)(\hat{x}_{k/k-1}, u_k)}{\delta \hat{x}_{k/k-1}} \quad \text{“the derivatives of the } r^{\text{th}} \text{ measurement”}$$

$$\text{Step 4: } S_k = H_k P_{k/k-1} H_k^T + R(r) \quad \text{“} S_k \text{ is a 1x1 matrix”}$$

$$\text{Step 5: } K_k = \frac{P_{k/k-1} H_k^T}{S_k}$$

$$\text{Step 6: } \hat{x}_{k/k} = \hat{x}_{k/k-1} + K_k \tilde{y}_k$$

$$\text{Step 7: } P_{k/k} = (I - K_k H_k) P_{k/k-1}$$

$$\text{Step 8: } \hat{x}_{k/k-1} = \hat{x}_{k/k} \quad , \quad P_{k/k-1} = P_{k/k} \quad \text{“reassign the posteriori to the a priori”}$$

}

Once the state estimator is controllable and observable, the system can be controlled with state feedback.

Controller

Position

The desired motor positions are determined by translating the fixed frame satellite position to the vehicle frame.

$$\begin{bmatrix} s_{x3} \\ s_{y3} \\ s_{z3} \end{bmatrix} = {}^3M_0 \begin{bmatrix} \cos(s_{el}) \cos(s_{az}) \\ \cos(s_{el}) \sin(s_{az}) \\ -\sin(s_{el}) \end{bmatrix}$$

Then, the desired motor positions are:

$$\begin{aligned} dp_{az} &= \text{atan2}(s_{y3}, s_{x3}) \\ dp_{el} &= -\text{atan}\left(\frac{s_{z3}}{\sqrt{s_{y3}^2 + s_{x3}^2}}\right) \\ dp_{sk} &= -\gamma \cos(\theta) \end{aligned}$$

Note that the function $\text{atan2}()$ needs to be used so that the quadrant of the azimuth position is known. But, the simpler $\text{atan}()$ can be used for elevation because it is assumed that elevation is between 0 and $\pi/2$.

Velocity

To reduce steady state errors due to angular velocities of the vehicle, position and velocity feedback will be used to move the antenna in the opposite directions of vehicle motion. First, the measured angular velocities, $(\dot{\gamma}, \dot{\beta}, \dot{\alpha})$, need to be translated into the vehicle frame. This has been done earlier in this paper for the gyroscopes.

$$\begin{bmatrix} g_x \\ g_y \\ g_z \end{bmatrix} = {}^3M_1 \begin{bmatrix} 0 \\ 0 \\ \dot{\alpha} \end{bmatrix} + {}^3M_2 \begin{bmatrix} 0 \\ \dot{\beta} \\ 0 \end{bmatrix} + \begin{bmatrix} \dot{\gamma} \\ 0 \\ 0 \end{bmatrix}$$

The motors must move opposite of these velocities. The azimuth motor is coincident with g_z and the elevation motor is coincident with g_y , but the skew motor is at the elevation angle.

$$\begin{aligned} dv_{az} &= -g_z \\ dv_{el} &= -g_y \\ dv_{sk} &= -(g_x \cos(\theta) - g_z \sin(\theta)) \end{aligned}$$

Command

Once the desired velocity and position of each motor is determined, the acceleration command to the motor can be calculated using a simple proportional plus derivative feedback scheme.

$$\begin{aligned}
 mc_{az} &= (dp_{az})Kp_{az} + (dv_{az} - mfv_{az})Kv_{az} \\
 mc_{el} &= (dp_{el} - \theta)Kp_{el} + (dv_{el} - \dot{\theta})Kv_{el} \\
 mc_{sk} &= (dp_{sk} - \phi)Kp_{sk} + (dv_{sk} - \dot{\phi})Kv_{sk}
 \end{aligned}$$

The position and velocity gains for each motor are tuned individually.

Chapter 3: Simulation Results

Because the commanded roll, pitch, and yaw of the motion base cannot be matched directly to the roll, pitch, and yaw of the dish, no comparison during simulation can be made for the full filter. This is because the dish must twist relative to the motion base in order for the system to run. But a smaller filter without the signal strength measurements can be simulated. The IMU can be oriented in the axes of the motion base so that the yaw, pitch, and roll of the motion base are the same as the yaw, pitch, and roll of the IMU. Then the smaller filter with no yaw and signal strength peak state can be run to estimate roll and pitch. Yaw is left out because it is unobservable without signal strength measurements.

Figure 8 shows the pitch and roll states, both commanded and estimated, over 120 seconds. The same IMU data as was used to determine the variances of the measurements is used to estimate the states in simulation.

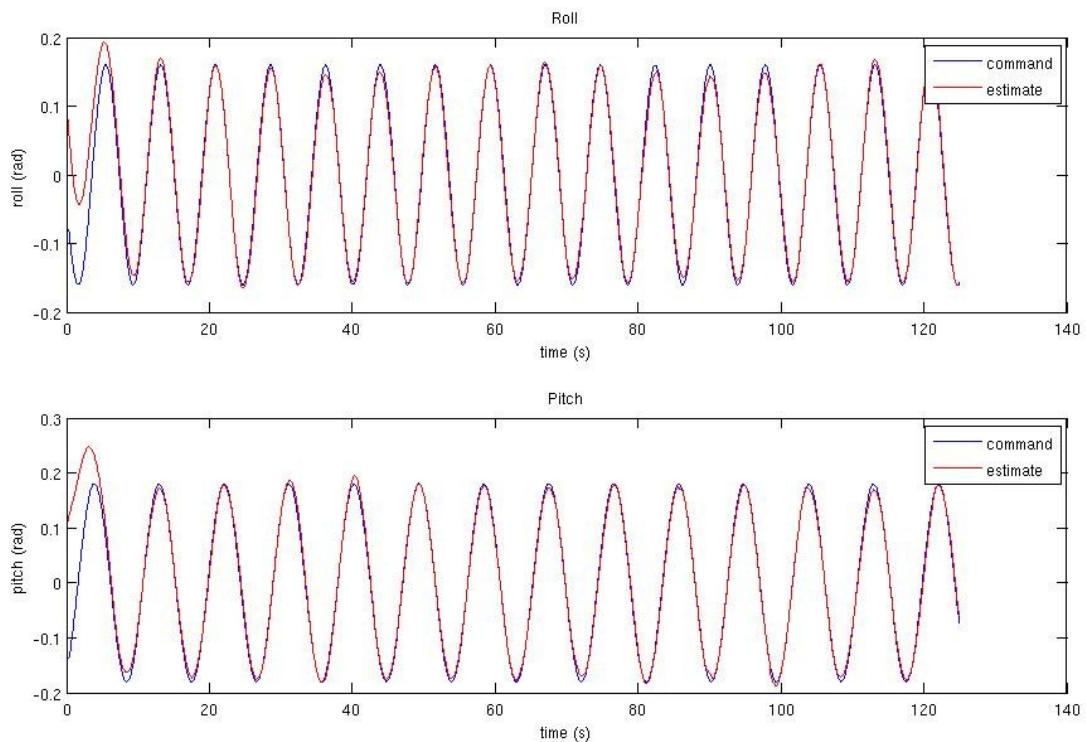


Figure 8: the estimated and commanded states of roll and pitch

Figure 9 shows the error between the commanded angles and the estimated angles. The red dashed lines show the 0.5 degree limit of error. All the states start out at 0.1 and converge on the correct

solution. Convergence occurs within 10 seconds and stays within approximately 0.7 degrees of error.

Figure 10 shows the model estimate of the mounting mast height of the antenna, R_z . It appears to level off about twice the value expected. The radius of rotation is difficult to observe despite the system being observable during the entire simulation, because of the relatively small accelerations it creates compared to gravity and the noise level of the accelerometer measurements. It may be reasonable to leave the R_z state out.

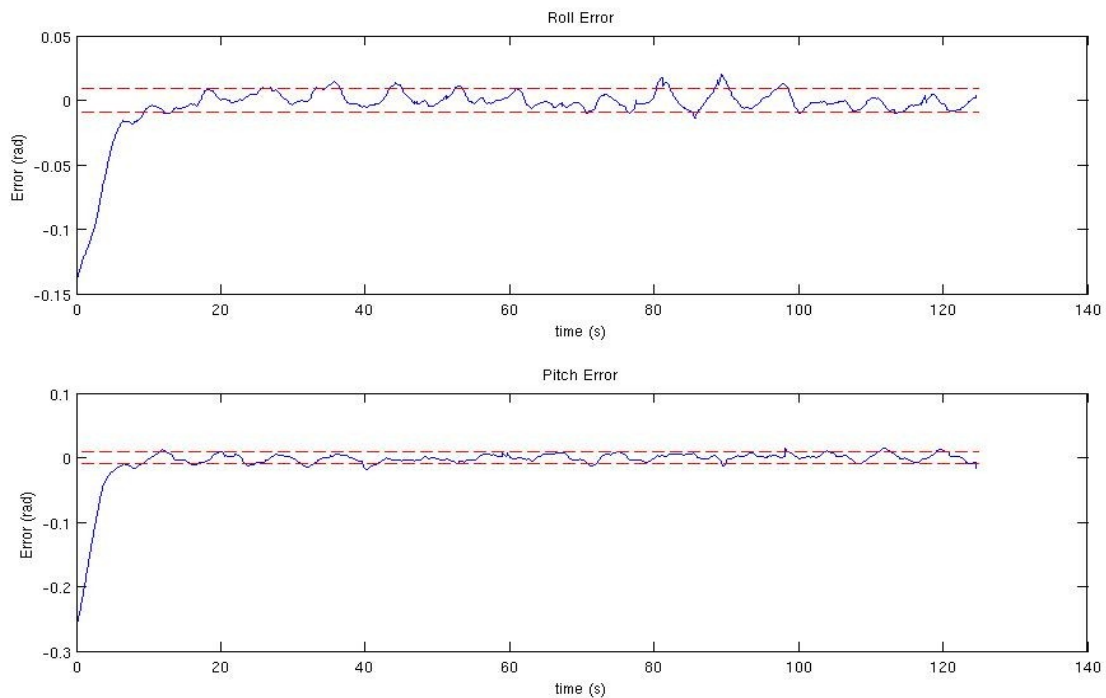


Figure 9: the error between the commanded and estimated roll and pitch during simulation

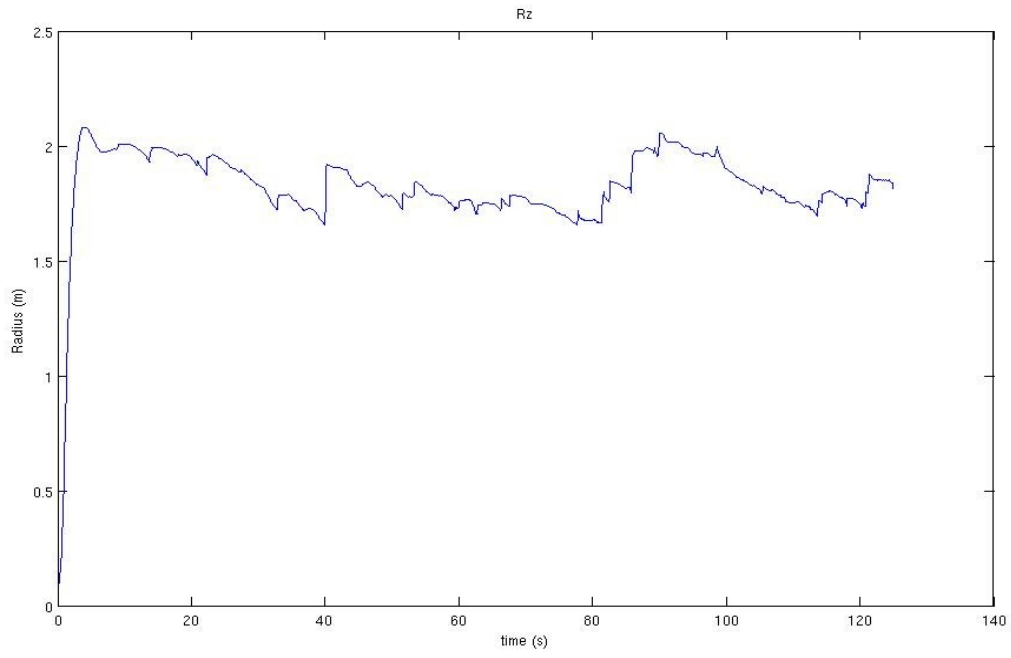


Figure 10: the R_z state during simulation

Chapter 4: Experimental Results

To test the performance of the whole system, the center of rotation of the motion base was moved to the intersection of the pointing vector and the elevation axis of the dish. This was done so the dish and laser would not translate relative to the LEDs on the wall. This was necessary because the only real output for the system was the position of the laser light on the wall.

The elevation precision is within the $\pm 0.5^\circ$. However, because yaw is not observable without the signal strength measurements and the signal strength measurements are not precise enough to measure a difference of 0.5° , the azimuth pointing angle varies by about 1° , depending on conditions. Below is a link to the system running in the lab. More definitive results are not available because the only real output is a laser shining on the wall.

[Lab Results Video](#)

Possibly, more definitive measurements could be taken with time lapsed photography showing all at once the locations of the laser light over a period of time. Then the error could be measured more precisely.

Chapter 5: Conclusions

There are several things that could be done to improve performance.

1. Using a narrower band reflector would result in more precision in the signal strength measurement being translated to the azimuth and elevation angles of the dish, because the measurements would be on a higher gradient portion of the signal curve. However, placing the signal strength measurements closer to the focal point of the dish would increase the signal to noise ratio. Optimizing these two effects could improve the performance of the system.
2. Use two IMUs. Two of each inertial measurements would help filter out noise in the measurements and get a better estimate of pitch and roll.
3. Generate an improved model for the signal strength, such as a Fourier transform version. The current Gaussian model does not take into account some of the eccentricities of the signal strength profile creating systematic errors and preventing the Kalman filter from performing optimally. However, there are problems in implementation. Computing two dimensional inverse FFTs (fast Fourier transforms) is computationally expensive compared to the Gaussian model. The Fourier model with terms out to the 5th harmonic would look something like Figure 11. The covariance between the Fourier model and the data in this case is 6.5429e-06, approximately one tenth that of the Gaussian model.

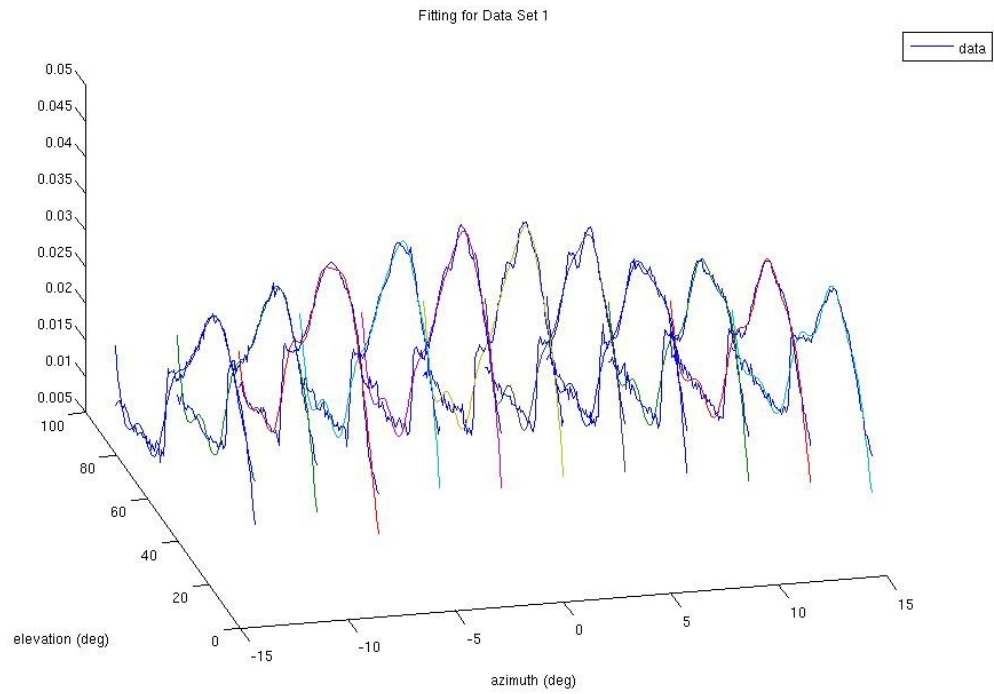


Figure 11: 5th harmonic Fourier model of the signal strength

[Fourier Model Demo](#)

Bibliography

3DM-GX1, <http://www.microstrain.com/inertial/3DM-GX1>, June 25, 2012

Analog Devices, ADIS16365 Inertial Measurement Unit, <http://www.analog.com/en/mems-sensors/mems-inertial-measurement-units/adis16365/products/product.html>, September 25, 2012

Aydogan Savran, Ramazan Tasaltin, Yasar Becerikli, “Intelligent Adaptive Nonlinear Flight Control for a High Performance Aircraft with Neural Networks”, ISA Transactions, Volume 45, Number 2, April 2006, pg. 225-247

“Barbara Reflectors for Bridgelux BXRA”, Ledil F'Form Optics, www.ledil.com, April 3, 2012

Cree Inc., XLamp MX-6S, <http://www.cree.com/led-components-and-modules/products/xlamp/discrete-nondirectional/xlamp-mx6>, September 26, 2012

Dan Simon, “Optimal State Estimation”, John Wiley & Sons, 2006

Girish Chowdhary, Ravindra Jategaonkar, “Aerodynamic parameter estimation from flight data applying extended and unscented Kalman filter ”, Aerospace Science and Technology 14 (2010), p. 106–117

Lionel Lapierre, “Robust Diving Control of an AUV ”, Ocean Engineering 36 (2009), p. 92–104

Seongpil Kim, Agus Budiyo, Jang-Ho Lee, DooHyun Kim, Kwang Joon Yoon, (2010), "Control system design and testing for a small-scale autonomous helicopter", Aircraft Engineering and Aerospace Technology, Vol. 82 Iss: 6 p. 353 – 359

Vishay, TEMD5010X01 Product Information, <http://www.vishay.com/photo-detectors/list/product-84679/>, September 26, 2012

Workhorse Navigator Doppler Velocity Log, <http://www.rdinstruments.com/navigator.aspx>, June 25, 2012

Appendix

Symbol Index

A - maximum amplitude of the signal strength

B - inputs to state update matrix

D - inputs to output matrix

F - state transition matrix in state space model

H - output matrix in state space model

I - identity matrix

K - Kalman gain matrix

K_p - controller gain for position

K_v - controller gain for velocity

aM_b - rotation matrix from frame b to frame a.

P - state covariance matrix

Q - state estimate covariance matrix

R - radius of rotation in the vehicle (3) frame

SS - signal strength measurement

T - period between time steps

a - acceleration measurement

az - azimuth location of signal strength measurement relative to nominal

dp - desired motor position

dv - desired motor velocity

el - elevation location of signal strength measurement relative to nominal

g - gyroscope measurement

$grav$ - acceleration due to gravity

m - motor command, acceleration

p - pointing position of the satellite dish

s - satellite position

u - system inputs

\hat{x} - state estimate

x - actual states

\hat{y} - output estimate

y - measured output

α - yaw

β - pitch

γ - roll

θ - elevation motor position

ϕ - skew motor position

az - azimuth angle of a vector, angle between x,y component and x axis.

el - elevation angle of a vector, negative of the angle between vector and x,y component

k - of current time step

$k+1$ - of next time step

$k-1$ - of last time step

$k+1/k+1$ - posteriori estimate

$k+1/k-1$ - a priori estimate

$k-1/k-1$ - posteriori estimate from last time step

sk - skew angle of a vector, right hand rotation angle

x - in the x axis

y - in the y axis

z - in the z axis

0 - in the fixed frame

1 - pertaining to signal strength measurement 1

2 - pertaining to signal strength measurement 2

3 - in the vehicle frame or pertaining to signal strength measurement 3

$$\dot{} = \frac{d}{dt}$$

$$\ddot{} = \frac{d^2}{dt^2}$$

Output Matrix Derivatives

$$\frac{dg_{xk}}{d\dot{\alpha}_k} = -\sin(\beta_k)$$

$$\frac{dg_{xk}}{d\beta_k} = -\dot{\alpha}_k \cos(\beta_k)$$

$$\frac{dg_{yk}}{d\dot{\alpha}_k} = \cos(\beta_k) \sin(\gamma_k)$$

$$\frac{dg_{yk}}{d\gamma_k} = -\dot{\beta}_k \sin(\gamma_k) + \dot{\alpha}_k \cos(\beta_k) \cos(\gamma_k)$$

$$\frac{dg_{yk}}{d\beta_k} = -\dot{\alpha}_k \sin(\beta_k) \sin(\gamma_k)$$

$$\frac{dg_{zk}}{d\dot{\alpha}_k} = \cos(\beta_k) \cos(\gamma_k)$$

$$\frac{dg_{zk}}{d\gamma_k} = \dot{\beta}_k \cos(\gamma_k) - \dot{\alpha}_k \cos(\beta_k) \sin(\gamma_k)$$

$$\frac{dg_{zk}}{d\beta_k} = -\dot{\alpha}_k \sin(\beta_k) \cos(\gamma_k)$$

$$\frac{da_{xk}}{d\dot{\beta}_k} = -R_{zk} \cos(\gamma_k)$$

$$\frac{da_{xk}}{d\dot{\alpha}_k} = -R_{zk} \cos(\beta_k) \sin(\gamma_k)$$

$$\frac{da_{xk}}{d\gamma_k} = -R_{zk} \cdot (-\dot{\beta}_k \sin(\gamma_k) + \dot{\alpha}_k \cos(\beta_k) \cos(\gamma_k))$$

$$\frac{da_{xk}}{d\beta_k} = R_{zk} \dot{\alpha}_k \sin(\beta_k) \sin(\gamma_k) - grav \cdot \cos(\beta_k)$$

$$\frac{da_{xk}}{dR_{zk}} = -(\dot{\beta}_k \cos(\gamma_k) + \dot{\alpha}_k \cos(\beta_k) \sin(\gamma_k))$$

$$\frac{da_{yk}}{d\dot{\alpha}_k} = -R_{zk} \sin(\beta_k)$$

$$\frac{da_{yk}}{d\gamma_k} = grav \cdot \cos(\beta_k) \cos(\gamma_k)$$

$$\frac{da_{yk}}{d\beta_k} = -R_{zk} \dot{\alpha}_k \cos(\beta_k) - grav \cdot \sin(\beta_k) \sin(\gamma_k)$$

$$\frac{da_{zk}}{d\dot{\gamma}_k} = 2R_{zk} (\dot{\gamma}_k - \dot{\alpha}_k \sin(\beta_k))$$

$$\frac{da_{zk}}{d\beta_k} = 2R_{zk} (\dot{\beta}_k \cos(\gamma_k) + \dot{\alpha}_k \cos(\beta_k) \sin(\gamma_k)) \cos(\gamma_k)$$

$$\frac{da_{zk}}{dR_{zk}} = ((\dot{\gamma}_k - \dot{\alpha}_k \sin(\beta_k))^2 + (\dot{\beta}_k \cos(\gamma_k) + \dot{\alpha}_k \cos(\beta_k) \sin(\gamma_k))^2)$$

The next derivatives are for the signal strength measurements. The derivatives with respect to γ , β , and α are all similar, with the difference being the derivatives of the p variables. The derivative with respect to γ is shown. The derivatives of the p variables with respect to γ , β , and α will be shown after the example derivative. The derivative is shown in steps from high level to lower level down to the state variables.

$$\begin{aligned} \frac{dSS_{nk}}{d\gamma_k} = & SS_{nk} \left[\frac{-(p_{az} + az_n \cos(p_{sk}) + el_n \sin(p_{sk}) - s_{az})}{\sigma^2} \left(\frac{dp_{az}}{d\gamma_k} - az_n \sin(p_{sk}) \frac{dp_{sk}}{d\gamma_k} + el_n \cos(p_{sk}) \frac{dp_{sk}}{d\gamma_k} \right) \right] \\ & + SS_{nk} \left[\frac{-(p_{el} + el_n \cos(p_{sk}) - az_n \sin(p_{sk}) - s_{el})}{\sigma^2} \left(\frac{dp_{el}}{d\gamma_k} - el_n \sin(p_{sk}) \frac{dp_{sk}}{d\gamma_k} - az_n \cos(p_{sk}) \frac{dp_{sk}}{d\gamma_k} \right) \right] \end{aligned}$$

$$\frac{dSS_{nk}}{dA_{zk}} = \exp \left[\frac{-(p_{az} + az_n \cos(p_{sk}) + el_n \sin(p_{sk}) - s_{az})^2}{2\sigma^2} - \frac{(p_{el} + el_n \cos(p_{sk}) - az_n \sin(p_{sk}) - s_{el})^2}{2\sigma^2} \right]$$

$$\frac{dp_{el}}{d\gamma_k} = \frac{-1}{\left(\frac{p_{0z}}{\sqrt{p_{0x}^2 + p_{0y}^2}} \right)^2 + 1} \frac{-p_{0x} p_{0z} \frac{dp_{0x}}{d\gamma_k} + p_{0x}^2 \frac{dp_{0z}}{d\gamma_k} + p_{0y} (p_{0y} \frac{dp_{0z}}{d\gamma_k} - p_{0z} \frac{dp_{0y}}{d\gamma_k})}{(p_{0x}^2 + p_{0y}^2)^{3/2}}$$

$$\frac{dp_{el}}{d\beta_k} = \frac{-1}{\left(\frac{p_{0z}}{\sqrt{p_{0x}^2 + p_{0y}^2}} \right)^2 + 1} \frac{-p_{0x} p_{0z} \frac{dp_{0x}}{d\beta_k} + p_{0x}^2 \frac{dp_{0z}}{d\beta_k} + p_{0y} (p_{0y} \frac{dp_{0z}}{d\beta_k} - p_{0z} \frac{dp_{0y}}{d\beta_k})}{(p_{0x}^2 + p_{0y}^2)^{3/2}}$$

$$\frac{dp_{el}}{d\alpha_k} = \frac{-1}{\left(\frac{p_{0z}}{\sqrt{p_{0x}^2 + p_{0y}^2}} \right)^2 + 1} \frac{-p_{0x} p_{0z} \frac{dp_{0x}}{d\alpha_k} + p_{0x}^2 \frac{dp_{0z}}{d\alpha_k} + p_{0y} (p_{0y} \frac{dp_{0z}}{d\alpha_k} - p_{0z} \frac{dp_{0y}}{d\alpha_k})}{(p_{0x}^2 + p_{0y}^2)^{3/2}}$$

$$\frac{dp_{az}}{d\gamma_k} = \frac{1}{\left(\frac{p_{0y}}{p_{0x}} \right)^2 + 1} \frac{p_{0x} \frac{dp_{0y}}{d\gamma_k} - p_{0y} \frac{dp_{0x}}{d\gamma_k}}{p_{0x}^2}$$

$$\frac{dp_{az}}{d\beta_k} = \frac{1}{\left(\frac{p_{0y}}{p_{0x}}\right)^2 + 1} \frac{p_{0x} \frac{dp_{0y}}{d\beta_k} - p_{0y} \frac{dp_{0x}}{d\beta_k}}{p_{0x}^2}$$

$$\frac{dp_{az}}{d\alpha_k} = \frac{1}{\left(\frac{p_{0y}}{p_{0x}}\right)^2 + 1} \frac{p_{0x} \frac{dp_{0y}}{d\alpha_k} - p_{0y} \frac{dp_{0x}}{d\alpha_k}}{p_{0x}^2}$$

$$\frac{dp_{0z}}{d\alpha_k} = 0$$

$$\frac{dp_{sk}}{d\gamma_k} = \cos(\theta)$$

$$\frac{dp_{sk}}{d\beta_k} = 0$$

$$\frac{dp_{sk}}{d\alpha_k} = 0$$

$$\frac{dp_{0x}}{d\gamma_k} = -\sin(\theta)(\sin(\alpha_k)\cos(\gamma_k) - \sin(\beta_k)\cos(\alpha_k)\sin(\gamma_k))$$

$$\frac{dp_{0x}}{d\beta_k} = -\sin(\beta_k)\cos(\alpha_k)\cos(\theta) - \sin(\theta)\cos(\beta_k)\cos(\alpha_k)\cos(\gamma_k)$$

$$\frac{dp_{0x}}{d\alpha_k} = -\cos(\beta_k)\sin(\alpha_k)\cos(\theta) - \sin(\theta)(\cos(\alpha_k)\sin(\gamma_k) - \sin(\beta_k)\sin(\alpha_k)\cos(\gamma_k))$$

$$\frac{dp_{0y}}{d\gamma_k} = \sin(\theta)(\cos(\alpha_k)\cos(\gamma_k) + \sin(\beta_k)\sin(\alpha_k)\sin(\gamma_k))$$

$$\frac{dp_{0y}}{d\beta_k} = -\sin(\theta)\cos(\beta_k)\sin(\alpha_k)\cos(\gamma_k) - \sin(\beta_k)\cos(\theta)\sin(\alpha_k)$$

$$\frac{dp_{0y}}{d\alpha_k} = \sin(\theta)(-\sin(\alpha_k)\sin(\gamma_k) - \sin(\beta_k)\cos(\alpha_k)\cos(\gamma_k)) + \cos(\beta_k)\cos(\theta)\cos(\alpha_k)$$

$$\frac{dp_{0z}}{d\gamma_k} = \cos(\beta_k)\sin(\theta)\sin(\gamma_k)$$

$$\frac{dp_{0z}}{d\beta_k} = -\cos(\beta_k)\cos(\theta) + \sin(\beta_k)\sin(\theta)\cos(\gamma_k)$$